Ion−Neutral Potential Models in Atmospheric Pressure Ion Mobility Time-of-Flight Mass Spectrometry IM(tof)MS

Wes E. Steiner,[†] William A. English,[‡] and Herbert H. Hill, Jr.*,[‡]

SAIC/Geo-Centers, Edgewood Chemical Biological Center Operations, Aberdeen Proving Grounds, Maryland USA, and Department of Chemistry, Washington State University, Pullman, Washington USA

Received: October 26, 2005; In Final Form: December 9, 2005

The ion mobilities and their respective masses of several classes of amines (primary, secondary, and tertiary) were measured by electrospray ionization atmospheric pressure ion mobility time-of-flight mass spectrometry IM(tof)MS. The experimental data obtained were comparatively analyzed by the one-temperature kinetic theory of Chapman−Enskog. Several theoretical models were used to estimate the collision cross-sections; they include the rigid-sphere, polarization-limit, 12-6-4, and 12-4 potential models.These models were investigated to represent the interaction potentials contained within the collision integral that occurs between the polyatomic ions and the neutral drift gas molecules. The effectiveness of these collision cross-section models on predicting the mobility of these amine ions was explored. Moreover, the effects of drift gas selectivity on the reduced-mass term and in the collision cross-section term was examined. Use of a series of drift gases, namely, helium, neon, argon, nitrogen, and carbon dioxide, made it possible to distinguish between mass effects and polarizability effects. It was found that the modified 12-4 potential that compensates for the center of charge not being at the same location as the centers of mass showed improved agreement over the other collision cross-section models with respect to experimental data.

1. Introduction

Since its introduction as a new dimension for gas chromatographic and mass spectrometric applications,[1] ion mobility spectrometry (IMS) has grown over the past couple of decades to become an important analytical separation technique.[2] IMS has been found to be straightforward to use, temporally fast, mechanically robust, and very sensitive to a wide range of applications (chemical warfare agent detection,[3] explosives residue detection,[4] illicit drug residue detection,[5] biological elucidation,[6] environmental monitoring,[7] workplace monitoring,[8] industrial process control,[9] and space shuttle cabin monitoring[10] to name a few). The success of many of these applications can be primarily contributed to three advances in IMS technology: (1) the development of an electrospray ionization (ESI) source that has significantly expand the breadth of compounds that could be measured by IMS to include nonvolatile molecules dissolved in aqueous environments,[11] (2) an increase in IMS resolving power efficiencies that exceed those of liquid chromatography (LC) and rivaled those of gas chromatography (GC),[12] and (3) the incorporation of IMS with mass spectrometry (MS) for the reliable identification of ions through their mass and fragmentation patterns.[13,14]

In addition to novel ionization methods, increased resolving power, and mass spectral identification, methods have been investigated in IMS to alter relative gas phase mobilities of ions. Experimentally it has been shown that the relative mobilities in IMS could be changed either by operating in an elevated electric field[15] or by employing a variety of different drift gases.[16] Rasulev et al., have shown that mixtures of ions can be selectively resolved in IMS by applying a direct current (DC) compensating voltage to a high frequency (<200 kHz) high asymmetric waveform dispersion voltage (~5000 V cm^{-1}).[17] In this case, only the ions that have the exactly right compensating voltage to balance the drift caused by the application of the asymmetric waveform will be resolved. More recently, Hill et al., has shown that not unlike similar chromatographic methods, which employ differing mobile and stationary phases to change selectivity, the use of different drift gases in IMS can directly affect the separation selectivity.[18] The utilization of different drift gases was initially investigated over two decades ago.[19] Since then, a whole host of investigations employing different drift gases have been explored having ranged from rare types of drift gases (sulfur hexafluoride, carbon tetrafluoride, nitrous oxide, ammonia, and neon) to a more commonly used variety (carbon dioxide, nitrogen, argon, and air).[20]

Surprisingly though, their has been minimal research involving the development of different levels of theory to relate fundamental characteristics of the ion−neutral interactions in the gas phase to the current applications of IMS mentioned above. Researchers have endeavored to predict the mobilities and related cross-sections for ions in a given drift gas from theoretical models for many years, but this has proven to be difficult due to the complexity of the mobility experiment. Traditionally, comparison between computer modeled structures and experimental collision cross-sections have been done with helium as the neutral drift gas (due to its weakly interacting low polarizability), which provides the simplest gas to derive a theoretical understanding of the interaction between an ion and the neutral drift gas.[21] For example, Karpas et al. showed that on the basis of rigorous IMS theory, the mobilities of a series

* Corresponding author. Tel, (509) 335-5648; Fax, (509) 335-8867; E-mail, hhhill@wsu.edu.
[†] Edgewood Chemical Biological Center Operations.
[‡] Washington State University.

10.1021/jp056158t CCC: $33.50
Published on Web 01/17/2006

of aliphatic amines could be predicted, specifically for the drift gas. On the basis of these theoretical curve fits, the predominating interactions of the ion−neutral collision were determined for several different drift gases.[22] Later, Hill et al., showed that by employing a less rigorous model they could estimate the ionic radii for several compounds in different drift gases.[23] This facilitated an empirical linear correlation between the drift gas polarizability and calculated ion radii, showing that ions with equivalent masses but different structures could still be separated in certain drift gases.

Although measurements of ion mobilities and theoretical models to interpret them abound, there is still a need for a systematic experimental study for the critical evaluation of the suitability of these models for polyatomic ions. In the present work, the mobilities of eighteen amines from three types of structural classes (primary, secondary, and tertiary) were measured by IMS. The experimental data obtained were analyzed with some commonly used theoretical models. The effectiveness of these models on predicting the mobility of these polyatomic ions was examined.

2. Theory

The general working principles of IMS technology have been described in detail elsewhere.[2] In short, an ion's characteristic mobility constant, K ($cm^2\ V^{-1}\ s^{-1}$), through a gas at uniform temperature, and pressure is defined by

$$K = \frac{v_d}{E} \tag{1}$$

where v_d ($cm\ s^{-1}$) is the ion's average drift velocity and E ($V\ cm^{-1}$) is the electric field intensity (provided that the field is weak) over the region of drift. Experimentally, ion mobility constants can be approximated by the amount of time, t_d (s), required for an ion to travel through a length, L (cm), of an IMS drift cell space using a rearranged form of eq 1, given as

$$K = \frac{L^2}{Vt_d} \tag{2}$$

where V is defined as the voltage drop applied across L. However, to take into account changing environmental conditions, it is practical to discuss an ion's mobility in terms of a standard or "reduced" mobility constant, K_0, defined as

$$K_0 = K\left(\frac{273.15}{T}\right)\left(\frac{P}{760}\right) \tag{3}$$

here, T (K), is the effective gas temperature and P (Torr) is the gas pressure in the drift cell region where the mobility, K, was obtained. Under these standard conditions of temperature (273.15 K) and pressure (760 Torr), the densities of the drift gas molecules are normalized.

Ion mobility has been studied with the use of a variety of theoretical techniques.[18] These fundamentally included momentum transfer theory, one-temperature kinetic theory (Chapman−Enskog), two-temperature kinetic theory, three-temperature kinetic theory, resonant charge exchange theory, polyatomic systems theory, and etc. Of these, the most commonly used formula for the mobility of ions drifting through a neutral gas in a weak electric field was based on the Chapman−Enskog theory given by

$$K = \left(\frac{3q}{16N}\right)\left(\frac{2\pi}{ukT_{eff}}\right)^{1/2}\left(\frac{1+\alpha}{\Omega_D(T_{eff})}\right) \tag{4}$$

where q is the charge of an ion with a mass of m, N is the neutral gas density with a formula weight of M, u is the reduced mass of the ion−neutral collision pair given by $u = m/M(m + M)$. T_{eff} is the effective temperature of the ions, $T_{eff} = T + M_t v_d^2/3k$, where M_t is the total mass of the colliding ion−neutral pairs (it is important to note that under experimentally low IMS field (where E/N is roughly 1 Td (Townsend, $10^{-17} cm^2$)) conditions, T_{eff} is essentially equal to the drift tube temperature.), k is the Boltzmann gas constant, α is a correction factor that is generally less than 0.02 for $m \geq M$, and Ω_D is the collision cross-section. A closer examination of eq 4 revealed the dependence of an ions mobility, K, on its mass, m, and how it enters directly in through the reduced-mass term, u, and through the collisional cross-section term, Ω_D. A result of this is that the heavier the ions are, with respect to the drift gas, the less likely the reduced mass term, u, will be a factor and the more likely the nature of the interaction potential that described the Ω_D would be the dominant term.

The collision cross-section term, Ω_D, depends on the nature of the interaction potential that was produced from the collision of the ion−neutral complex. Basically, there are two types of contributions to this interaction potential. These involved either an infinite potential (that acknowledges the induced-dipole−induced-dipole interaction associated with van der Waal interactions) or a point charge-induced dipole between an ion and a neutral molecule. In either case the basic definition is as follows:

$$\Omega_D = \pi r_m^{\,2}\, \Omega_{ave}^{(1,1)}(T^*) \tag{5}$$

where πr^2 and $\Omega_{ave}^{(1,1)}(T^*)$ is the hard-core cross section and dimensionless collision integral that depends on the ion−neutral interaction potential and is a function of the dimensionless temperature, $T^* = kT/\epsilon_0$. Here, ϵ_0 is the depth of the minimum in the potential surface and r_m is the position of that minimum as defined by $\epsilon_0 = e^2\alpha_p/[3r_m^4(1 - a^*)^4]$, where e is the ion charge, α_p is the polarizability of the drift gas molecules, and a^* is the reduced core diameter as a function of the separation between the center of charge and the center of mass of the ion defined as a divided by the position of the potential surface minimum r_m. Moreover, it has been previously shown that by making some simplifying assumptions about the nature of the ion−neutral interactions, several theoretical models (rigid-sphere, polarization-limit, 12-6-4, and 12-4) can be used to estimate the resultant collision cross-sections.[24]

As a first approximation (not taking into account ion−neutral forces), the ion and neutral molecule interaction can be treated or modeled as a rigid-sphere that basically accounts for the collision cross-section of both the ion and neutral drift gas as rigid spheres:

$$\Omega_D = \pi(r_i + r_n)^2 \tag{6}$$

where r_i and r_n are the radii of the ion and neutral molecule, respectively. In the polarization-limit approach, it was assumed that the neutral molecule had no permanent dipole or quadrupole moments, and the only interactions arose from a "long-range" point charge-induced dipole (or ion-induced dipole potential). This interaction potential, $V(r)$, described as

$$V(r) = \frac{q^2\alpha}{2r^4} \tag{7}$$

is a function of the polarizability, α_p, of the neutral molecule, which will vary as a function of the distance, r, between the ion and the neutral molecule. Here the collision cross-section

TABLE 1: Formula Weight, Polarizability, and Radii for the Five Neutral Drift Gases Employed

drift gas	formula weight[a] (Da)	polarizability[b] (Å^3)	radii[c] (Å)	radii[e] (Å)	radii[f] (Å)
helium (He)	4.00260	0.205	1.40	1.03	3.38
neon (Ne)	20.1797	0.396	1.54	n.d.	n.d.
nitrogen (N_2)	28.0134	1.740	n.d.[d]	1.73	5.77
argon (Ar)	39.948	1.641	1.88	1.67	5.69
carbon dioxide (CO_2)	44.0098	2.911	n.d.	2.02	6.57

[a] Mass of longest lived isotopes.[32] [b] Values of 1.0 Å^3 = 10^{-24} cm^3 from literature.[33] [c] van der Waals.[34] [d] n.d.: not determined. [e] Rigid-sphere model.[21] [f] Polarization-limit model.[35]

is

$$\Omega_D \propto \left(\frac{q^2\alpha_p}{kT}\right)^{1/2} \tag{8}$$

The formula weight, polarizability, and radii for each neutral drift gas used in these experiments are summarized in Table 1. Once the ion and the neutral molecule approach each other at short ranges, repulsive and attractive interactions between them become important. When both a "short-range" repulsive and attractive term is added to the "long-range" polarization-limit model shown in eq 7 discussed above, the interaction potential is modified to a form of a 12-6-4 potential:

$$V(r) = \frac{\epsilon_0}{2}\left[(1+\gamma)\left(\frac{r_m}{r}\right)^{12} - 4\gamma\left(\frac{r_m}{r}\right)^{6} - 3(1-\gamma)\left(\frac{r_m}{r}\right)^{4}\right] \tag{9}$$

here, γ is a parameter used to regulate the strength of the induced dipole interaction. Unfortunately, all of these models described above implicitly assumed that an ion and a neutral behaved as if the centers of repulsion, attraction, and polarization were all located at the centers of mass of both species. Although this was a reasonable assumption for small ions and small neutral molecules, it does not hold for relatively large, complex ions. The failure of these models to quantitatively explain mobility data has been demonstrated in detail elsewhere.[25,26] Moreover, because our studies involve the use of larger polyatomic ions (e.g., mass and collisional cross-section), it was important to consider an alternate model that acknowledged uncertainties in the location of the center of charge may not be located near its center of mass. Therefore, the parameter a (as defined for eq 5) was introduced to express this separation of the center of mass from the center charge. The type of interaction potential used in most cases was found to be the 12-4 potential as follows:

$$V(r) = \frac{\epsilon_0}{2}\left[\left(\frac{r_m - a}{r - a}\right)^{12} - 3\left(\frac{r_m - a}{r - a}\right)^{4}\right] \tag{10}$$

where ϵ_0, a, and r_m were defined above. Evaluation of the collision cross-sections from these interaction potentials (eqs 9 and 10) has been shown to be difficult for any but the simplest of ion−neutral interactions, and thus has never been rigorously evaluated.[25] Therefore, approximations are generally used when collision cross-section calculations are performed. The collision cross-sections dimensionless parameter, $\Omega_{ave}^{(1,1)}(T^*)$ term found in eq 5 can now be expanded to include fluctuations of reduced ion temperature at both low $[1/(T^*)^{1/2}]$ and high $[1/(T^*)^{1/6}]$ temperatures to take the form of

$$\Omega_D = \pi r_m^{\,2}\,\Omega_{ave}^{(1,1)}(T^*) = \pi r_m^{\,2}\left[A + \frac{B}{(T^*)^{1/2}} + \frac{C}{(T^*)^{1/6}}\right] \tag{11}$$

TABLE 2: Parameters for Ω_D of Eq 11

	12-6-4 potential model				12-4 potential model		
γ	A	B	C	$a^* = a/r_m$	A	B	C
0	0.6763	2.0697	−1.3251	0.0	0.6508	1.9498	−1.2344
0.25	0.5375	1.7359	−0.9185	0.1	0.5378	1.5961	−0.7920
0.5	0.3668	1.3391	−0.4307	0.2	0.4613	1.2766	−0.4254
0.75	0.2042	0.8262	0.1734	0.3	0.4207	0.9939	−0.1343
1.0	0.4052	1.0282	−0.2463	0.4	0.4144	0.7458	0.0846
				0.5	0.4419	0.5343	0.2303
				0.6	0.5015	0.3590	0.3055
				0.7	0.5913	0.2196	0.3122
				0.8	0.7066	0.1144	0.2601

TABLE 3: Mass, Ions, and Reduced Mobility Constant (K_o) Values in Several Different Drift Gases over a Range of Common Amine Classes

			K_o (cm^2 V^{-1} s^{-1})				
compound	mass	ions	He	Ne	N_2	Ar	CO_2
		Primary					
propylamine	60	$(M+H)^+$	3.6	3.01	2.49	2.24	1.68
pentylamine	88	$(M+H)^+$	3.21	2.62	2.12	1.97	1.50
heptylamine	116	$(M+H)^+$	2.83	2.27	1.87	1.73	1.35
nonylamine	144	$(M+H)^+$	2.43	1.98	1.63	1.53	1.22
undecylamine	172	$(M+H)^+$	2.15	1.76	1.45	1.35	1.11
tridecylamines	200	$(M+H)^+$	1.86	1.56	1.25	1.18	0.98
		Secondary					
dimethylamine	46	$(M+H)^+$	3.49	3.07	2.49	2.27	1.64
diethylamine	74	$(M+H)^+$	3.09	2.67	2.15	1.97	1.42
dipropylamine	102	$(M+H)^+$	2.74	2.30	1.87	1.72	1.28
dibutylamine	130	$(M+H)^+$	2.39	1.98	1.65	1.53	1.16
dipentylamine	158	$(M+H)^+$	2.15	1.79	1.49	1.37	1.08
dihexylamine	186	$(M+H)^+$	2.02	1.65	1.39	1.26	1.04
		Tertiary					
trimethylamine	60	$(M+H)^+$	3.43	2.84	2.39	2.21	1.60
triethylamine	102	$(M+H)^+$	2.83	2.37	1.95	1.80	1.36
tripropylamine	144	$(M+H)^+$	2.36	1.98	1.63	1.50	1.19
tributylamine	186	$(M+H)^+$	1.98	1.64	1.40	1.28	1.06
tripentylamine	228	$(M+H)^+$	1.73	1.44	1.23	1.13	0.95
trihexylamine	270	$(M+H)^+$	1.51	1.27	1.09	1.01	0.85

where the constants A, B, and C have been determined by performing regression analysis to published tabular data[26] and are shown in Table 2. Although the variables in eq 11 can be solved empirically by successive mathematical iterations, the accuracy of this approach has not been found to be as good as just simply using tabulated data.

3. Experimental Section

3.1. Chemicals and Solvents. Eighteen total amines in three classes: primary (propyl, pentyl, heptyl, nonyl, undecyl, tridecyl), secondary (dimethyl, diethyl, dipropyl, dibutyl, dipentyl, dihexyl), and tertiary (trimethyl, triethyl, tripropyl, tributyl, tripentyl, trihexylamine) were purchased from Sigma Aldrich Chemical Co. (St. Louis, MO) as purum (≥99.5%) standards. Stock solutions for these primary, secondary, and tertiary amines were prepared in ESI solvent (47.5% water, 47.5% methanol, 5% acetic acid) at concentrations of 1000 ppm (1000 μg/mL). Further dilutions of these stock solutions with ESI solvent ranged from 100 ppb to 100 ppm (0.1 μg/mL to 100 μg/mL), depending upon the experiment. The HPLC grade ESI solvents (water, methanol, acetic acid) were purchased from J. T. Baker (Phillipsburgh, NJ).

3.2. Instrumentation. The IM(tof)MS instrument used was constructed at Washington State University where the fundamental components (ESI source; APIMS drift tube; pressure interface; TOFMS analyzer; and data acquisition system) and modes of operation have been previously described in considerable detail.[3,14] Thus, only a brief outline of a typical experimental sequence is provided. A continuous flow (5.0 μL/min) of solvent

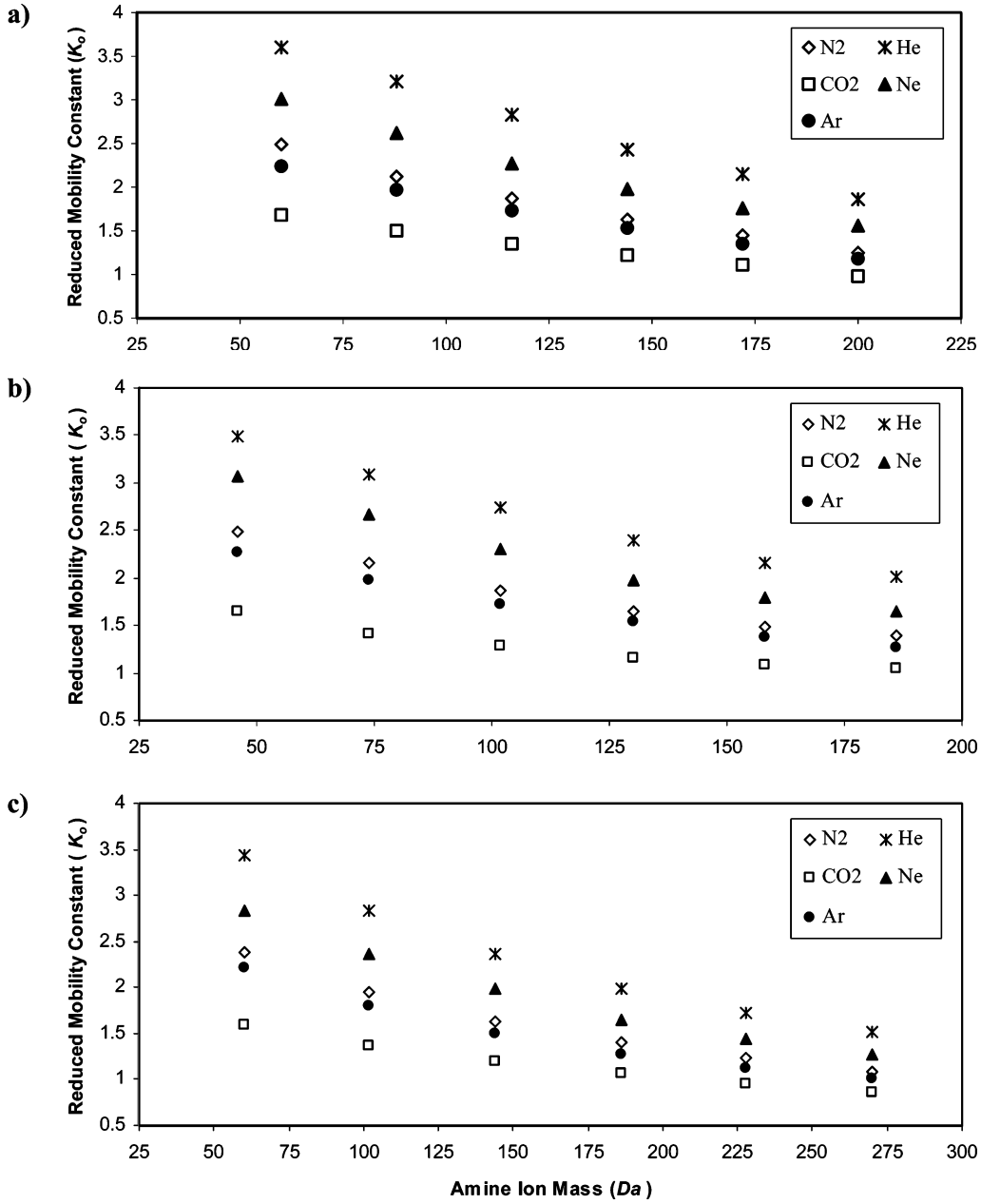

Figure 1. Reduced mobility constants, K_o, of (a) primary (propyl, pentyl, heptyl, nonyl, undecyl, tridecyl), (b) secondary (dimethyl, diethyl, dipropyl, dibutyl, dipentyl, and dihexyl), and (c) tertiary (trimethyl, triethyl, tripropyl, tributyl, tripentyl, and trihexyl) amines as a function of their relative ion masses in five different drift gases (helium, neon, nitrogen, argon, and carbon dioxide).

was electrosprayed in the positive ion mode with a needle voltage of +3.5 kV with respect to the target screen of the APIMS. The APIMS was divided into two regions, the desolvation (8.0 cm in length) and the drift (18.0 cm in length) regions, that were separated by a Bradbury−Nielsen style ion gate.[27] Desolvated ions typically drifted through the 473 K APIMS tube under a weak uniform electric field (472 V/cm), which facilitated separation based upon differing analyte mobility constants. A counter current flow of preheated nitrogen drift gas was introduced at the end of the drift region at a rate of 1.0 L/min. Ions exiting the APIMS drift tube (696 Torr) traversed a pressure interface (1.5 Torr) where parent and daughter ions could be transported through a series of lenses into the TOFMS (4.0×10^{-6} Torr) for analysis.

Data acquisition for this experimental setup consisted of a timing sequence that was comprised of a real-time two-dimensional matrix of simultaneous mobility drift and mass flight times. Ions were typically gated for 0.2 ms into the drift region at a frequency of 50 Hz. This allowed for a maximum of 20 ms for the APIMS mobility data to be acquired. The TOFMS extraction frequency was set to 50 kHz, which provided a mass spectrum that consisted of ions with flight times up to 20 μs. Therefore, within each 20 ms mobility time window there were effectively 1000 TOF extractions. The APIMS ion gate, TOFMS extractor, and TOFMS time-to-digital converter were all triggered by a personal computer (PC) based timing controller. Synchronization of this electronic hardware was facilitated by the use of a dual Pentium III workstation running Ionwerks two-dimensional acquisition software.[28] Experimental data acquisitions were typically run for 1 min to provide clear ion statistics. This ensured that the effects of ionization efficiency and ion transmission were not a limiting factor when determining limits of detection. Spectral compilations of data once acquired were then exported into both 2D Transform[29] and 3D NoeSYS[30] software for processing.

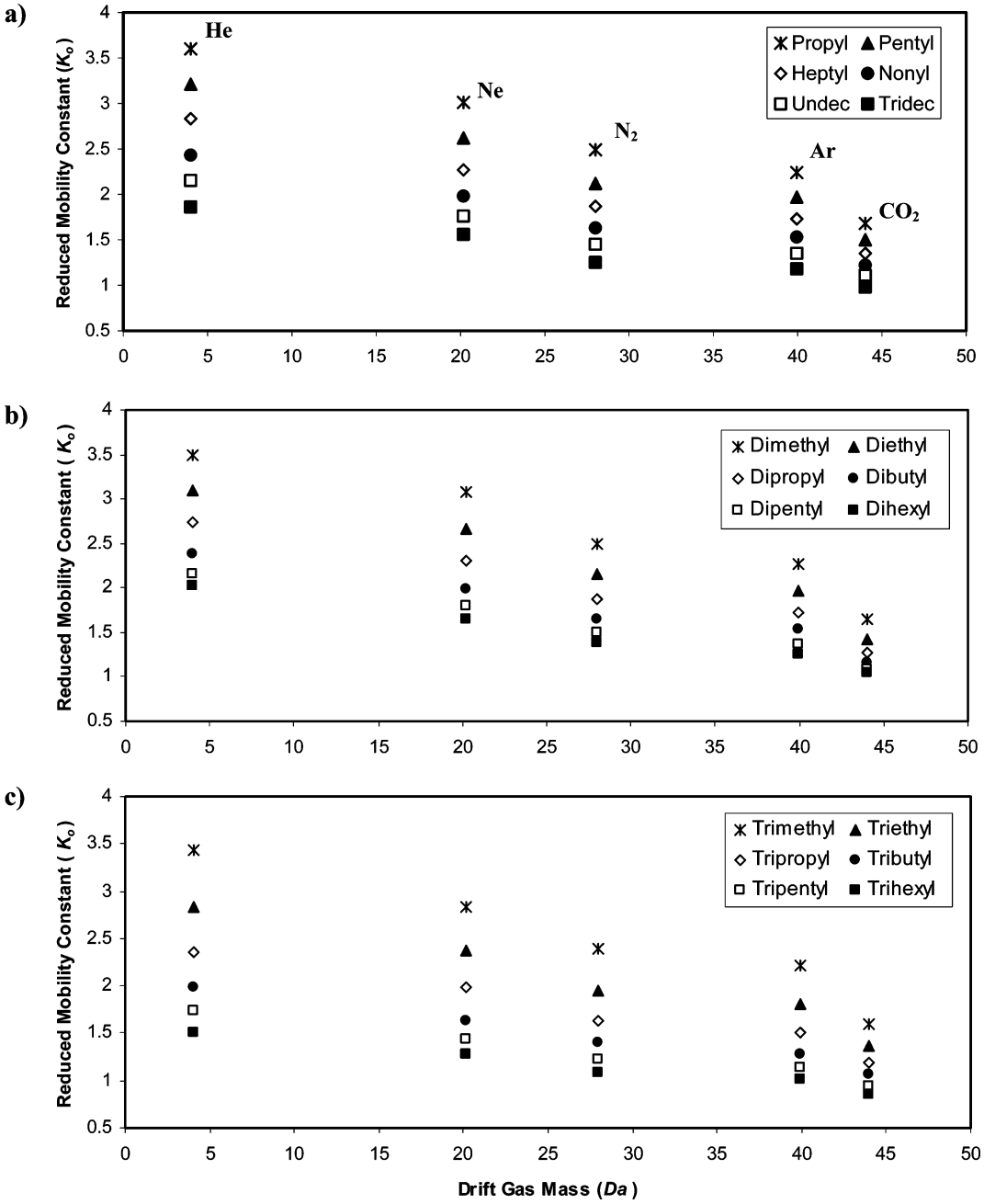

Figure 2. Reduced mobility constants, K_o, of (a) primary (propyl, pentyl, heptyl, nonyl, undecyl, tridecyl), (b) secondary (dimethyl, diethyl, dipropyl, dibutyl, dipentyl, and dihexyl), and (c) tertiary (trimethyl, triethyl, tripropyl, tributyl, tripentyl, and trihexyl) amines as a function of five different drift gases (helium, neon, nitrogen, argon, and carbon dioxide) mass.

4. Results and Discussion

4.1. Mobility of Ions in Varying Drift Gases. Reduced mobility constants, K_o, of (a) primary (propyl, pentyl, heptyl, nonyl, undecyl, tridecyl), (b) secondary (dimethyl, diethyl, dipropyl, dibutyl, dipentyl, and dihexyl) and (c) tertiary (trimethyl, triethyl, tripropyl, tributyl, tripentyl, and trihexyl) amines as a function of their relative ion masses in five different drift gases (helium, neon, nitrogen, argon, and carbon dioxide) are tabulated in Table 3. As can be seen by the table, the fastest and slowest mobilities (K_o = 3.6 and 0.85 $cm^2\ V^{-1}\ s^{-1}$) were obtained by propylamine and trihexylamine in helium and carbon dioxide, respectively. Similarly, dimethylamine had a reduced mobility of 3.49 $cm^2\ V^{-1}\ s^{-1}$ in helium and 1.64 $cm^2\ V^{-1}\ s^{-1}$ in carbon dioxide. Slower reduced mobilities were expected in carbon dioxide as it had the largest calculated radius of all the drift gases investigated, as shown in Table 1. In all cases, amine ions had the shortest mobility drift times in helium and the longest in carbon dioxide, with neon, nitrogen and argon being intermediate, respectively. This relative drift time to drift gas trend has been observed elsewhere for other compounds.[22,23]

4.2. Mobility Dependence on Ion Mass. As the mass of the amine ions increased, with respect to their drift gases, the mobility of the ion decreased (i.e., smaller reduced mobility constants, K_o) as they drifted through the APIMS tube. Figure 1, shows the K_o values of (a) primary (propyl, pentyl, heptyl, nonyl, undecyl, tridecyl), (b) secondary (dimethyl, diethyl, dipropyl, dibutyl, dipentyl, and dihexyl) and (c) tertiary (trimethyl, triethyl, tripropyl, tributyl, tripentyl, and trihexyl) amines as a function of their relative ion masses in five different drift gases (helium, neon, nitrogen, argon, and carbon dioxide). Here, for example in Figure 1a, the reduced mobility of 3.6 and 1.86 $cm^2\ V^{-1}\ s^{-1}$ for propylamine (60 Da) and tridecylamine (200

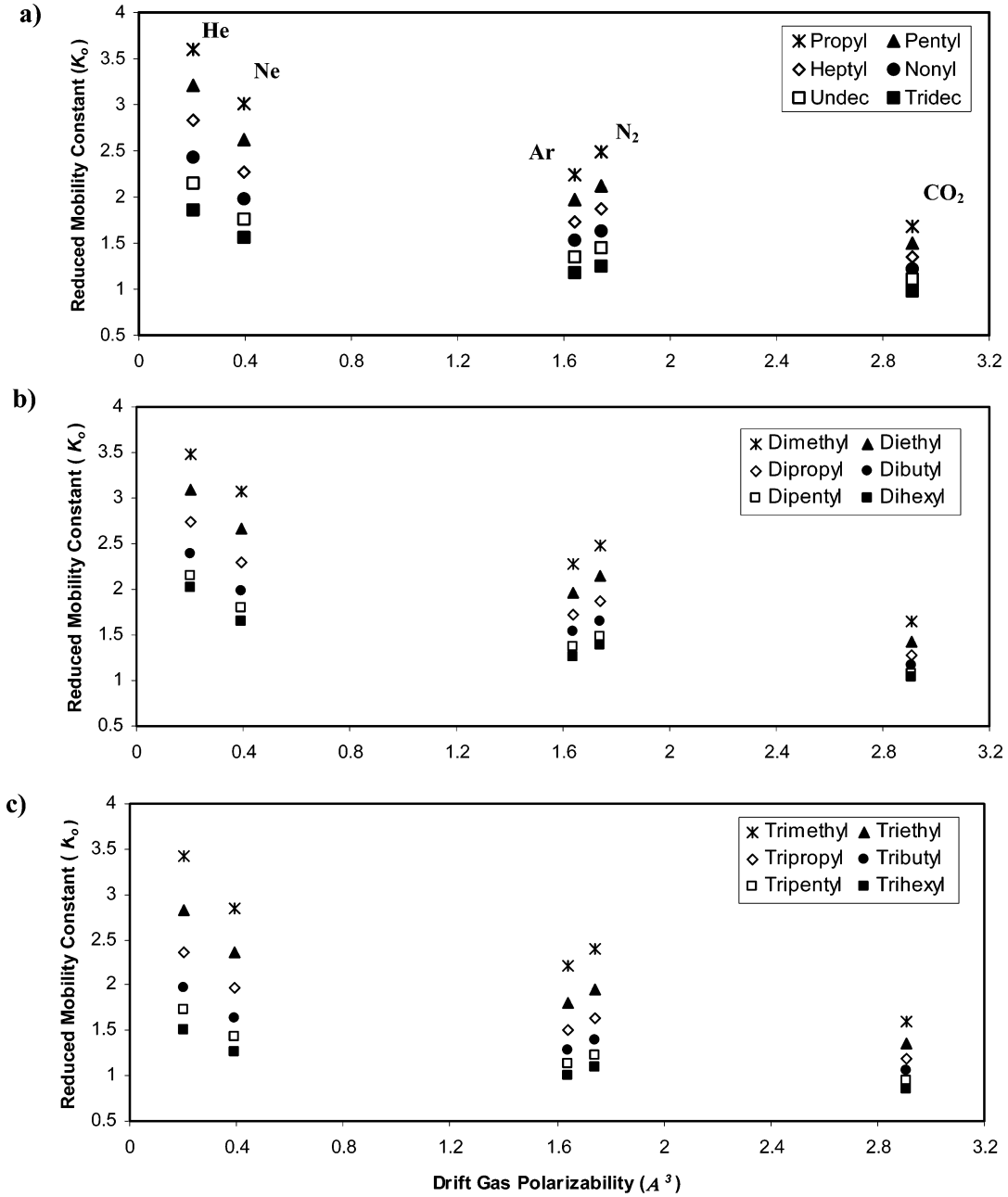

Figure 3. Reduced mobility constants, K_o, of (a) primary (propyl, pentyl, heptyl, nonyl, undecyl, tridecyl), (b) secondary (dimethyl, diethyl, dipropyl, dibutyl, dipentyl, and dihexyl), and (c) tertiary (trimethyl, triethyl, tripropyl, tributyl, tripentyl, and trihexyl) amines as a function of five different drift gases (helium, neon, nitrogen, argon, and carbon dioxide) polarizability.

Da) in helium (4.0 Da), respectively, indicated that the mass dependence of the amine ions mobility entered in through the collisional cross-section term, Ω_D, and to some degree through the reduced mass of the ion−neutral collision pair, u, of eq 4. The result of this can be seen in all of Figure 1's data: the heavier the ions were with respect to the drift gas (i.e., $m > M$) they were drifting through, the less likely the reduced mass term, u, would be a factor and the more likely the nature of the interaction potential that described the collisional cross-section term, Ω_D, would become important. Eventually, when higher ion masses is reached, the reduced mass becomes practically invariable with further increase of ion mass. This behavior can start to be seen by a closer examination of the spectra in Figure 1. As amine ions of all classes began to approach values of elevated mass, they began to converge toward a horizontal asymptote. Needless to say, more data points would be required to show the complete asymptotic convergence of the reduced mass.

4.3. Mobility Dependence on Drift Gas Mass. Similarly, as the case above, as the mass of the neutral drift gas increased, with respect to a given amine ion, the mobility of the amine ion decreased as it drifted through the APIMS tube. Figure 2, shows the reduced mobility constants, K_o, of (a) primary (propyl, pentyl, heptyl, nonyl, undecyl, tridecyl), (b) secondary (dimethyl, diethyl, dipropyl, dibutyl, dipentyl, and dihexyl) and (c) tertiary (trimethyl, triethyl, tripropyl, tributyl, tripentyl, and trihexyl) amines as a function of five different neutral drift gas (helium, neon, nitrogen, argon, and carbon dioxide) masses. Here, for example, in Figure 2a, the reduced mobility of 3.6 and 1.68 $cm^2\ V^{-1}\ s^{-1}$ for propylamine (60 Da) in helium (4.0 Da) and carbon dioxide (44 Da), respectively, indicated that the mass

TABLE 4: Theoretical versus Experimental Reduced Mobility Constants[a]

compound	K_o ($cm^2\ V^{-1}\ s^{-1}$) He	N_2	CO_2
	Primary		
propylamine	**3.60**, 3.68, 1.73, 4.54, 3.62*	**2.49**, 2.51, 1.14, 3.50, 2.50*	**1.68**, 1.75, 0.81, 2.73, 1.66*
pentylamine	**3.21**, 3.30, 1.65, 4.16, 3.22*	**2.12**, 2.15, 0.93, 3.11, 2.12*	**1.50**, 1.62, 0.74, 2.57, 1.51*
heptylamine	**2.83**, 2.85, 1.43, 3.80, 2.83*	**1.87**, 1.87*, 0.89, 2.74, 1.89	**1.35**, 1.38, 0.69, 2.42, 1.34*
nonylamine	**2.43**, 2.44*, 1.16, 3.39, 2.45	**1.63**, 1.65, 0.75, 2.54, 1.64*	**1.22**, 1.34, 0.61, 2.29, 1.22*
undecylamine	**2.15**, 2.19, 0.95, 3.13, 2.15*	**1.45**, 1.47, 0.64, 2.43, 1.46*	**1.11**, 1.20, 0.55, 2.19, 1.08*
tridecylamines	**1.86**, 1.88*, 0.85, 2.85, 1.89	**1.25**, 1.29, 0.56, 2.49, 1.25*	**0.98**, 1.08, 0.49, 2.04, 0.99*
	Secondary		
dimethylamine	**3.49**, 3.55, 1.42, 4.43, 3.50*	**2.49**, 2.50, 1.19, 3.48, 2.49*	**1.64**, 1.73, 0.79, 2.67, 1.64*
diethylamine	**3.09**, 3.12, 1.30, 4.03, 3.10*	**2.15**, 2.16*, 0.94, 3.24, 2.18	**1.42**, 155, 0.70, 2.57, 1.41*
dipropylamine	**2.74**, 2.74*, 1.19, 2.77, 2.76	**1.87**, 1.91, 0.83, 2.72, 1.87*	**1.28**, 1.34, 0.61, 2.27, 1.29*
dibutylamine	**2.39**, 2.41, 1.09, 3.35, 2.39*	**1.65**, 1.67*, 0.80, 2.59, 1.68	**1.16**, 1.21, 0.55, 2.13, 1.16*
dipentylamine	**2.15**, 2.18, 1.03, 3.14, 2.16*	**1.49**, 1.54, 0.70, 2.44, 1.51*	**1.08**, 1.13, 0.51, 2.05, 1.06*
dihexylamine	**2.02**, 2.03*, 0.88, 3.00, 2.04	**1.39**, 1.44, 0.66, 2.34, 1.39*	**1.04**, 1.10, 0.50, 2.00,1.05*
	Tertiary		
trimethylamine	**3.43**, 3.47, 1.65, 4.38, 3.45*	**2.39**, 2.43, 1.05, 3.36, 2.40*	**1.60**, 1.65, 0.76, 2.54, 1.58*
triethylamine	**2.83**, 2.85, 1.30, 3.78, 2.84*	**1.95**, 2.02, 0.87, 2.90, 1.95*	**1.36**, 1.43, 0.65, 2.31, 1.36*
tripropylamine	**2.36**, 2.38, 1.19, 3.34, 2.36*	**1.63**, 1.66*, 0.79, 2.55, 1.68	**1.19**, 1.23, 0.57, 2.16, 1.17*
tributylamine	**1.98**, 1.98*, 0.99, 2.91, 1.99	**1.40**, 1.44, 0.65, 2.32, 1.40*	**1.06**, 1.11, 0.55, 2.03, 1.06*
tripentylamine	**1.73**, 1.74, 0.87, 2.65, 1.73*	**1.23**, 1.28, 0.59, 2.46, 1.24*	**0.95**, 1.01, 0.45, 1.90, 0.96*
trihexylamine	**1.51**, 1.54, 0.77, 2.43, 1.51*	**1.09**, 1.18, 0.52, 2.00, 1.12*	**0.85**, 0.99, 0.50, 1.84, 0.85*

[a] For all entries the first (bold) number is the experimental value, the second is the rigid-sphere value, the third is the polarization-limit value, the fourth is the 12-6-4 value and the fifth is the 12-4 value. Asterisks indicate the best theoretical fit.

dependence of the neutral drift gas atoms also entered in through both the collisional cross-section term, Ω_D, and the reduced mass of the ion−neutral collision pair, u, of eq 4. This trend can also be seen in all of Figure 2's data: the more the neutral drift gas atoms increased in mass, M, with respect to the amine ion's mass, m (i.e., $m \geq M$), again the less likely the reduced mass term, u, became a factor and the more likely the nature of the interaction potential that described the collisional cross-section term, Ω_D, became important. This behavior can be clearly seen from a different perspective by a closer examination of the spectra in Figure 2. As amine ions began to approach values of elevated neutral drift gas mass, they began to show convergent behavior as correspondingly seen in Figure 1.

4.4. Mobility Dependence on Drift Gas Polarizability. On first inspection, it seemed that the lower in polarizability the neutral drift gas was, the more the amine ions increased in mobility as they drifted through the APIMS tube. This trend was similar to the dependence shown above with decreasing neutral drift gas mass. Figure 3 outlines the reduced mobility constants, K_o, of (a) primary (propyl, pentyl, heptyl, nonyl, undecyl, tridecyl), (b) secondary (dimethyl, diethyl, dipropyl, dibutyl, dipentyl, and dihexyl) and (c) tertiary (trimethyl, triethyl, tripropyl, tributyl, tripentyl, and trihexyl) amines as a function of five different drift gases (helium, neon, nitrogen, argon, and carbon dioxide) polarizability. However, upon closer examination, it can be seen that the data for argon and nitrogen did not follow the trend generated by the reduced mobility versus neutral drift gas plot seen in Figure 2. In fact, if changes in reduced mobility were strictly a function of polarizability, the amine ions would have traveled faster in nitrogen than in argon. This, however, was clearly not the case. These data demonstrate the complexity of predicting ion mobility in various drift gases. As shown above in eq 4, mobility is related not only to the collision cross-section (which contains the polarizability term, α_p, of the neutral drift gas) but also to the reduced mass of the ion−neutral collision pair. Although the polarizability of argon is slightly lower than that of nitrogen, the mass of argon is significantly more. Thus, it appears that reduced mass was the dominant term that controlled the mobility of amine ions in argon relative to that in nitrogen. This trend can be seen in Figure 3a, where the reduced mass terms for propylamine (60 Da) in argon (0.67) versus propylamine in nitrogen (0.47) was a difference of 0.20. In comparison tridecylamine (200 Da) in argon (0.20) versus tridecylamine in nitrogen (0.14) produced a reduced mass difference of 0.06. This indicated that the mass dependence of the reduced mass term for the heavier tridecylamine was beginning to become more important then the effects of polarizability. Conversely, this also indicated that the reduced mass of propylamine in argon versus nitrogen, 0.20, could be attributed to both reduced mass effects and polarizability.

4.5. Theoretical Mobility of Ions. The experimental data obtained above were comparatively analyzed by the one-temperature kinetic theory of Chapman−Enskog. Where several theoretical models were used to estimate the collision cross-sections of this theory, they included the rigid-sphere (eq 6), polarization-limit (eq 8), 12-6-4 (eq 11), and 12-4 (eq 11) models. Moreover, with the combination and rearrangement of eqs 2 and 3, to yield

$$K_0 = \left(\frac{L^2}{Vt_d}\right)\left(\frac{273.15}{T}\right)\left(\frac{P}{760}\right) \tag{12}$$

and eqs 3 and 4 to give

$$K_0 = \left(\frac{3q}{16N}\right)\left(\frac{2\pi}{ukT_{eff}}\right)^{1/2}\left(\frac{1+\alpha}{\Omega_D(T_{eff})}\right)\left(\frac{273.15}{T}\right)\left(\frac{P}{760}\right) \tag{13}$$

these equations show the expanded forms of eq 3 that governs the reduced mobility of gas-phase ions could be generated. Here, the link between experimental (eq 12) and theoretical (q 13) gas-phase ion transportation data could be simultaneously compared. This not only provided a theoretical avenue to explore the feasibility of calculated reduced mobility values but also had the added benefit of compensating for environmental fluctuations that could arise from experimental practice.

To that end, Mathcad Professional[31] was used to integrate eqs 6, 8, 11, 12, and 13 for both the experimental and theoretical conditions used in this study. The theoretical reduced mobility

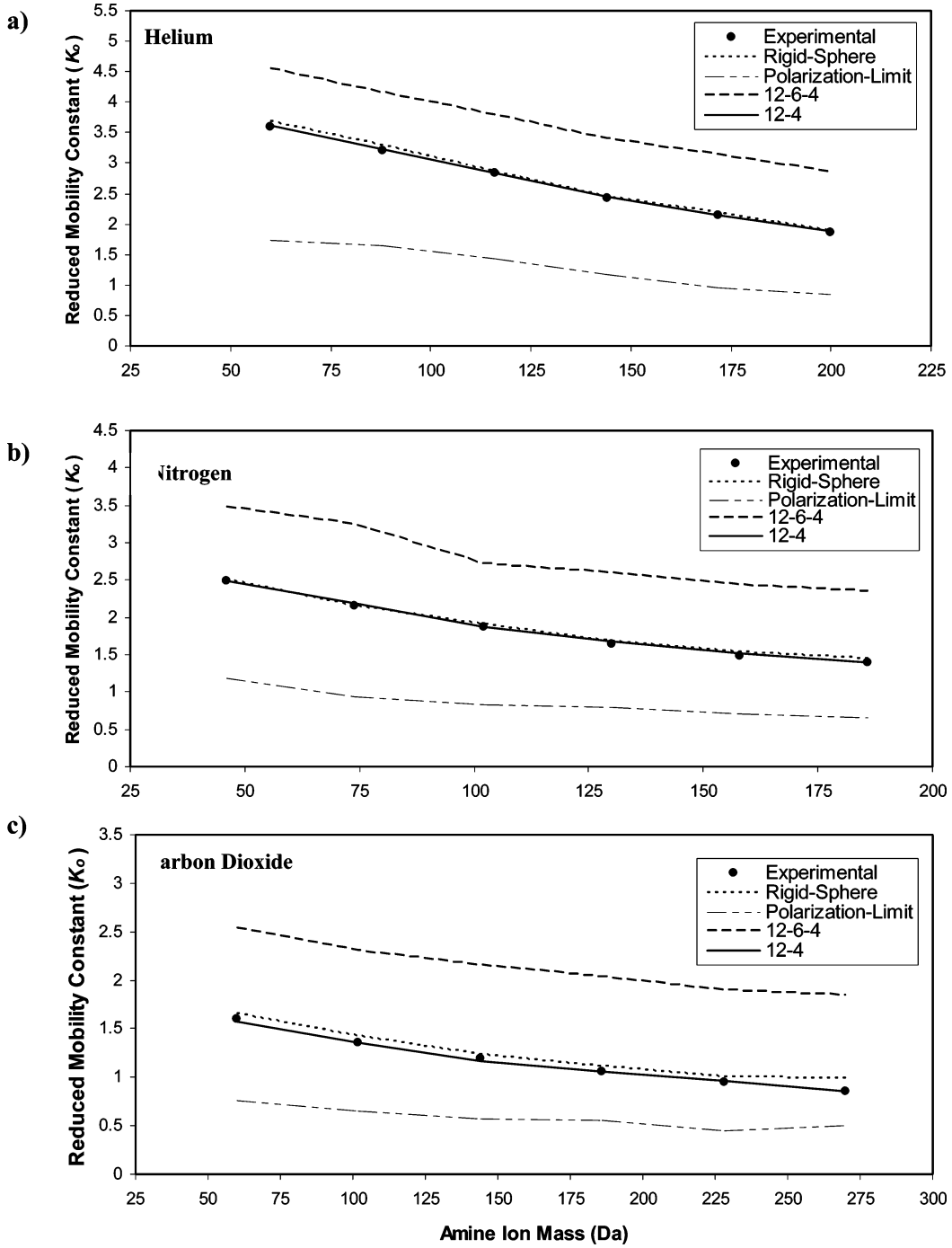

Figure 4. Comparison of experimental, rigid-sphere, polarization-Limit, 12-6-4, and 12-4 reduced mobility constants, K_o, of (a) primary (propyl, pentyl, heptyl, nonyl, undecyl, tridecyl), (b) secondary (dimethyl, diethyl, dipropyl, dibutyl, dipentyl, and dihexyl), and (c) tertiary (trimethyl, triethyl, tripropyl, tributyl, tripentyl, and trihexyl) amines as a function of their relative ion masses in helium, nitrogen and carbon dioxide, respectively.

constants deduced from the equations were then tabulated in Table 4 for comparison with experimental data. These data in Table 4 show that both the polarization limit and 12-6-4 models seemed to perform the worst. This intuitively was to be expected because the assumptions underlying both the above approaches limited their applicability. For example, the polarizability of a neutral drift gas, in the polarization limit model, depended on the limit where the electric field $E \rightarrow 0$ and the temperature $T \rightarrow 0$. Generally, these models have been used with limited success in some cases where small, generally monatomic, ions drift through a neutral, in most cases inert, gas such as helium.[25] The 12-6-4 model made the assumption that the center of mass of the ion was also assumed to be the center of its charge. Unfortunately, when dealing with relatively large polyatomic ions, this no longer was valid. However, with further inspection of some of the data in Table 4 in graphical form (Figure 4) it could be clearly seen that both the rigid-sphere and 12-4 models performed better in the comparison of experimental, reduced mobility constants, K_o, of (a) primary (propyl, pentyl, heptyl, nonyl, undecyl, tridecyl), (b) secondary (dimethyl, diethyl, dipropyl, dibutyl, dipentyl, and dihexyl) and (c) tertiary (trimethyl, triethyl, tripropyl, tributyl, tripentyl, and trihexyl) amines as a function of their relative ion masses in helium, nitrogen and carbon dioxide, respectively. Although the rigid-sphere model performed adequately in this study (especially for the helium drift gas in Figure 4a), it should be noted that it has

traditionally shown limited capabilities to reproduce experimental data for more complex ions.[24] The 12-4 model performed the best overall, regardless of what drift gas was employed. This mainly was attributed to the fact that the 12-4 model acknowledged uncertainties in the location of the charge. Thus, allowing for the amine ions charge to resonate throughout its molecular structure.

5. Conclusions

The ion mobilities of several classes of amines (primary, secondary, and tertiary) were successfully measured by electrospray ionization atmospheric pressure ion mobility time-of-flight mass spectrometry IM(tof)MS. The experimental data obtained were comparatively analyzed by the one-temperature kinetic theory of Chapman−Enskog, where the fundamental relationships describing the collision cross-sections of this theory were presented. Basically, it was found that the ion charge to center of mass distribution, which used an effective core diameter that expressed the separation of these two centers, could significantly affect the collision process and thus the measured ion mobilities. This was manifested by the 12-4 model providing the best overall theoretical fit to experimental data. Empirically, the observation was also made that an inverse relationship did in fact exist between the observed reduced mobility constants and the mass and polarizability of the neutral drift gas. This was facilitated by ions primarily achieving an increased mobility in drift gases that was smaller in mass and lower in polarizability (i.e., helium) than in drift gases that were larger in mass and higher in polarizability (i.e., carbon dioxide). In the cases where the ions were much larger in mass than the drift gas, the reduced mass term was found to be effectively the mass of the ion and, therefore, would not contribute greatly to the separation of the very large mass ions. Meaning, ion mobility spectrometry tended to separate low molecular weight ions on the basis of both their mass and collision cross-section (where polarizability effects come into play), and higher molecular weight compounds primarily on the basis of their collision cross-sections.

Acknowledgment. This work was supported in part by GeoCenters Incorporated (Grant #40853CMGC3173).

References and Notes

(1) Cohen, M. J.; Karasek, F. W. *J. Chromatogr. Sci*. **1970**, *8*, 330.
(2) Carr, T. W. *Plasma Chromatography*; Plenum Publishing Corporation: New York, 1984. Collins, D. C.; Lee, M. L. *Anal. Bioanal. Chem*. **2002**, *372*, 66. Eiceman, G. A.; Karpas, Z. *Ion Mobility Spectrometry*, 2nd ed.; CRC Press: Boca Raton, FL, 2005.
(3) Steiner, W. E.; Clowers, B. H.; Matz, L. M.; Siems, W. F.; Hill, H. H., Jr. *Anal. Chem.* **2002**, *74*, 4343−4352. Steiner, W. E.; Haigh, P. B.; Clowers, B. H.; Hill, H. H. *Anal. Chem.* **2003**, *75*, 6068−6078. Steiner, W. E.; Klopsch, S. J.; English, W. A.; Hill, H. H., Jr. *Anal. Chem.* **2005**, *77* (15), 4792−4799.
(4) Asbury, G. R.; Klasmeier, J.; Hill, H. H., Jr. *Talanta* **2000**, *50*, 1291.
(5) Wu, C.; Siems, W. F.; Hill, H. H., Jr. *Anal. Chem.* **2000**, *72*, 396.
(6) Hoaglund-Hyzer, C. S.; Lee, Y. J.; Counterman, A. E.; Clemmer, D. E. *Anal. Chem.* **2002**, *74*, 992.
(7) Clowers, B. H.; Steiner, W. E.; Dion, H. M.; Matz, L. M.; Tam, M.; Tarver, E. E.; Hill, H. H., Jr. *Field Anal. Chem. Tech*. **2001**, *5*, 302.
(8) Gordon, G.; Pacey, G.; Bubnis, B.; Laszewski, S.; Gaines, J. *Chem. Oxid*. **1997**, *4*, 23.
(9) Reategui, J.; Bacon, T. Vapors. *Proc. Control Qual*. **1992**, *3*, 209.
(10) Palmer, P. T.; Limero, T. F. *J. Am. Soc. Mass Spectrom*. **2001**, *12*, 656.
(11) Geinec, J.; Mack, L. L.; Nakamae, K.; Gupta, C.; Kumar, V.; Dole, M. *Biomedical Mass Spectrom.* **1984**, *11*, 259. Shumate, C. B.; Hill, H. H., Jr. *Anal. Chem.* **1989**, *61*, 601. Smith, R. D.; Loo, J. A.; Ogorazalek, R. R.; Busman, M. *Mass. Spectrom. Rev.* **1991**, *10*, 359. Wittmer, D. P.; Chen, Y. H.; Luckenbill, B. K.; Hill, H. H., Jr. *Anal. Chem.* **1994**, *66*, 2348. Chen, Y. H.; Hill, H. H., Jr.; Wittmer, D. P. *J. Microcolumn Sep.* **1994**, *6*, 515. Chen, Y. H.; Siems, W. F.; Hill, H. H., Jr. *Anal. Chim. Acta* **1996**, *334*, 75.
(12) Wu, C.; Siems, W. F.; Rasulev, U.K.; Nazarov, E. G.; Hill, H. H., Jr. Mass identification of Mobility Separated Ions Formed by Electropsray Ionixation and Surface Ionization. *Proceedings of the 45th ASMS Conference on Mass Spectromtery and Aplied Topics*; ASMS: 1997; p 376. Dogourd, P. H.; Hudgins, R. R.; Clemmer, D. E.; Jarrold, M. F. *Rev. Sci. Instrum*. **1997**, *68*, 1122. Wu, C.; Siems, W. F.; Asbury, G. R.; Hill, H. H., Jr. *Anal. Chem.* **1998**, *70*, 4929. Srebalus, C. A.; Li, J.; Marshall, W. S.; Clemmer, D. E. *Anal. Chem.* **1999**, *71*, 3918. Asbury, G. R.; Hill, H. H., Jr. *J. Microcolumn Sep*. **2000**, *12*, 172. Matz, L. M.; Clowers, B. H.; Steiner, W. E.; Siems, W. F.; Hill, H. H., Jr. *Anal. Chem. Technol*. **2001**, *5*, 3028. Wu, C.; Steiner, W. E.; Tornatore, P. S.; Matz, L. M.; Siems, W. F.; Atkinson, D. A.; Hill, H. H., Jr. *Talanta* **2002**, *57*, 123.
(13) Karasek, F. W.; Hill, H. H.; Kim, S. H. *J. Chromatogr. Sci*. **1976**, *117*, 327. (b) Kim, S. H.; Spangler, G. E. *Anal. Chem.* **1985**, *57*, 1890. Kim, S. H.; Spangler, G. E. *Anal. Chem.* **1986**, *58*, 1269. Liu, Y.; Clemmer, D. E. *Anal. Chem.* **1997**, *69*, 2504. Wu, C.; Siems, W. F.; Asbury, G. R.; Hill, H. H., Jr. *Anal. Chem.* **1998**, *70*, 4929. Purves, R. W.; Guevremont, R.; Day, S.; Pipich, C. W.; Matyjaszcayk, M. S. *Rev. Sci. Instrum*. **1998**, *69*, 4094. Hoaglund, C. S.; Valentine, S. J.; Sporleder, C. R.; Reilly, J. P.; Clemmer, D. E. *Anal. Chem*. **1998**, *70*, 2236. Henderson, S. C.; Valentine, S. J.; Counterman, A. E.; Clemmer, D. E. *Anal. Chem.* **1999**, *71*, 291. 59. Hoaglund-Hyzer, C. S.; Clemmer, D. E. *Anal. Chem.* **2001**, *73*, 177. Srebalus Barnes, C. A.; Hilderbrand, A. E.; Valentine, S. J.; Clemmer, D. E. *Anal. Chem.* **2002**, *74*, 26.
(14) Steiner, W. E.; Clowers, B. H.; Fuhrer, K.; Gonin, M.; Matz, L. M.; Siems, W. F.; Schultz, A. J.; Hill, H. H., Jr. *Rapid Commun. Mass Spectrom*. **2001**, *15*, 2221.
(15) Guevremont, R.; Purves, R. W. *Rev. Sci. Instrum*. **1999**, *70*, 1370. Purves, R. W.; Guevermont, R. *Anal. Chem.* **1999**, *71*, 2346. Barnet, D. A.; Ells, B.; Guevremont, R.; Purves, R. W.; Viehland, L. A. *J. Am. Soc. Mass Spectrom.* **2000**, *11*, 1125.
(16) Beegle, L. W.; Kanik, I.; Matz, L.; Hill, H. H. *Anal. Chem.* **2001**, *73*, 3028.
(17) Buryakov, I. A.; Krylov, E. V.; Makas, A. L.; Nazarov, E. G.; Pervukhin, V. V.; Rasulev, U. Kh. *Pis'ma Zh. Tekh. Fiz.* **1991**, *17*, 60−65. Buryakov, I. A.; Krylov, E. V.; Nazarov, E. G.; Rasulev, U. Kh. *Int. J. Mass Spectrom. Ion Processes* **1993**, *128*, 143.
(18) Matz, L. M.; Beegle, L. W.; Kanik, I.; Hill, H. H. *J. Am. Soc. Mass Spectrom.* **2001**, *13*, 300.
(19) Revercomb, H. E.; Mason, E. A. *Anal. Chem.* **1975**, *47*, 970.
(20) Ellis, H. W.; Pai, R. Y.; Gatland, I. R.; McDaniel, E. W.; Wernlund, R.; Cohen, M. J. *Anal. Chem.* **1976**, *64*, 3935. Sennhauser, E. S.; Armstrong, D. A. *Can. J. Chem*. **1978**, *56*, 2337. Carr, T. W. *Anal. Chem.* **1979**, *51*, 705. Sennhauser, E. S.; Armstrong, D. A. *Can. J. Chem.* **1980**, *58*, 231. Rokushika, S.; Hatano, H.; Hill, H. H., Jr. *Anal. Chem.* **1986**, *58*, 361. Berant, Z.; Karpas, Z.; Shahal, O. *J. Phys. Chem.* **1989**, *93*, 7529. Yamashita, T.; et al. *Nucl. Instrum. Methods Phys.* **1989**, *A283*, 709.
(21) Shvartsburg, A. A.; Jarrold, M. F. *Chem. Phys. Let*. **1996**, *261*, 86. Mesleh, M. F.; Hunter, J. M.; Shvartsburg, A. A.; Schatz, G. C.; Jarrold, M. F. *J. Phys. Chem*. **1996**, *100*, 16082. Shvartsburg, A. A.; Mashkevich, S. V.; Siu, M. K. W. *J. Phys. Chem. A* **2000**, *104*, 9448.
(22) Karpas, Z.; Barant, Z. *J. Phys. Chem.* **1989**, *93*, 3021.
(23) Asbury, G. R.; Hill, H. H. *Anal. Chem.* **2000**, *72*, 580.
(24) Mason, E. A.; McDaniel, E. W. *Transport Properties of Ions in Gases*; John Wiley & Son, Inc.: New York, 1988.
(25) Mason, E. A.; O'Hara, H.; Smith, F. J. *J. Phys. B: At. Mol. Phys*. **1972**, *5*, 169. Mason, E. A. Schamp, H. W. *Ann. Phys*. **1958**, *4*, 233. Karpas, Z.; Berant, Z. *J. Am. Chem. Soc*. **1989**, *11*, 3819.
(26) Spangler, G. E. *Field Anal. Chem. Tech*. **2000**, *4* (5), 255.
(27) Bradbury, N. E.; Neilson, R. A. *Phys. Rev*. **1936**, *49*, 388.
(28) Ionwerks 2-D, Ionwerks Inc., Houston TX, 2001.
(29) Transform V3.4, Fortner Software LLC, Serling, VA, 1998.
(30) NoeSYS V2.4, Research Systems Inc., Boulder, CO, 2000.
(31) Mathcad Professional V7.0, MathSoft Inc., Cambridge MA, 2000.
(32) Commission on Atomic Weights and Isotopic Abundances report for the International Union of Pure and Applied Chemistry. In Isotopic Compositions of the Elements 1989. *Pure Appl. Chem.* **1998**, *70*, 217. [Copyright 1998 IUPAC].
(33) Weast, R. C.; Lide, D. R.; Astle, M. J.; Beyer, W. H. *CRC Handbook of Chemistry and Physics*, 70th ed.; CRC Press: Boca Raton, FL, 1989.
(34) Bondi, A. *J. Phys. Chem.* **1964**, *68*, 441.
(35) Beegle, L. W.; Kanik, I.; Matz, L.; Hill, H. H., Jr. *Int. J. Mass Spectrom*. **2002**, *216*, 257.